

Dynamical estimates of chaotic systems from Poincaré recurrences

M. S. Baptista,^{1,2} Dariel M. Maranhão,³ and J. C. Sartorelli³

*¹Institute for Complex Systems and Mathematical Biology,
King's College, University of Aberdeen,
AB24 3UE Aberdeen, United Kingdom*

*²Centro de Matemática da Universidade do Porto,
Rua do Campo Alegre 687, 4169-007 Porto, Portugal*

*³Institute of Physics, University of São Paulo,
Rua do Matão, Travessa R, 187, 05508-090 SP, Brasil*

Abstract

We show a function that fits well the probability density of return times between two consecutive visits of a chaotic trajectory to finite size regions in phase space. It deviates from the exponential statistics by a small power-law term, a term that represents the deterministic manifestation of the dynamics. We also show how one can quickly and easily estimate the Kolmogorov-Sinai entropy and the short-term correlation function by realizing observations of high probable returns. Our analyzes are performed numerically in the Hénon map and experimentally in a Chua's circuit. Finally, we discuss how our approach can be used to treat data coming from experimental complex systems and for technological applications.

Observing how long a dynamical system takes to return to some state is one of the simplest ways to model and quantify its dynamics from data series. In this work, we describe a simple way to extract some relevant invariant quantities of a chaotic system by using recurrence times, in particular Poincaré recurrences that measure the time interval for a system to return to a configuration close to its initial state. Part of this work is dedicated to apply the theoretical results proposed by [Pinto *et al.* arXiv:0908.4575] to calculate the Kolmogorov-Sinai entropy and the decay of correlation of the experimental Chua’s circuit when the returns are measured in “large” size regions in phase space. Another part is dedicated to study how the deviation (from the exponential form) of the density of the first Poincaré returns can be used to detect deterministic manifestations in chaotic systems. Finally, we discuss how our approach can be used to treat data coming from experimental complex systems and for technological applications.

I. INTRODUCTION

Chaotic systems have simultaneously a stochastic [1] and a deterministic dynamical characters [2]. Single trajectories are predictable (deterministic) for a short-term evolution and unpredictable for a long-term evolution (stochastic). While the stochastic character is associated with an exponential decay of correlations and information about the actual state is rapidly lost as the trajectory evolves, the deterministic character is associated to a power-law decay of correlations and information about the actual state is lost as the system is evolved, but in a rather slower fashion.

A relevant question that arises when dealing with data coming from complex systems is whether manifestations of chaotic behavior can be detected in the data [3] so that one can construct deterministic models. One wishes to come up with a dynamical description of the data, but due to the sensitivity dependence on initial conditions of chaotic systems one is prompt to adopt a probabilistic approach in order to reveal the underlying dynamics of the system from statistical averages [4]. A promising tool of analysis is provided by the statistics of the Poincaré recurrence time (PRT) [5] which measures the time interval between two consecutive visits of a trajectory to a finite size region in phase space.

Many relevant quantifiers of low-dimensional chaotic systems can be obtained by the

statistical properties of the PRTs. The purpose of the present work is to apply some results from Ref. [6] and to propose other theoretical approaches to easily identify deterministic and stochastic manifestations in dissipative strongly chaotic systems by using the PRTs of chaotic trajectories to regions of finite size [7], considering only short return times. These later two conditions constraining our analyzes are devoted to suitably apply our approaches to realistic physical situations: the resolution to measure returns as well as the time frame to realize the experiment is finite.

By chaotic systems, we mean non-uniformly hyperbolic systems. We focus the analyzes on the Hénon map and on an experiment, the Chua's circuit, but we also present results coming from the logistic map.

We first present the theoretical framework to be used in Secs. II,III,IV, and V. Then, in Sec. VI, we apply this approach to analyze the Hénon map and the experimental Chua's circuit. We also work with the Logistic map in Appendix A.

In Sec. II, we present a continuous function, ρ_F that fits well the probability distribution for the PRTs to regions of finite size. The many parameters of ρ_F are theoretically estimated in Sec. III. Further, we show how to use these parameters to quantify how stochastic or deterministic the considered system is, under the perspective of the PRTs. Concerning the coefficient of the power-law term (responsible for the deviation of ρ_F from the Poisson distribution), a first approximation furnishes that it is inversely proportional to the average return time. The longer (shorter) is the average return time, the smaller (larger) the power-law term, and the more stochastic (more deterministic) the PRTs.

In Sec. IV, we succinctly describe how to calculate the Kolmogorov-Sinai (KS) entropy, denoted by H_{KS} , in terms of the number of unstable periodic orbits (UPOs) and of the frequency with which the PRT happen. Then, we explain how H_{KS} can be calculated in typical physical situations, when the information about the UPOs is unknown and the only available information is the frequency with which a high probable PRT with short length happens. Notice that this frequency can be easily measured even if only a few return times are observed because faster returns are more probable.

Alternative methods to calculate the correlation entropy, K_2 , a lower bound of H_{KS} , and to calculate H_{KS} from time series were proposed in Refs. [8, 9]. In Ref. [8] K_2 is calculated from the correlation decay and in Ref. [9] by the determination of a generating partition of phase space that preserves the value of the entropy. But while the method in

Ref. [8] unavoidably suffers from the same difficulties found in the proper calculation of the fractal dimensions from data sets, the method in Ref. [9] requires the knowledge of the generating partitions, information that is not trivial to be extracted from complex data. The advantage of the theoretical approach used is its simplicity. As one can see in Eq. (19), the only information required is the frequency with which high probable PRTs happen in some regions of the phase space.

In Sec. V, we show how the PRTs can be used to calculate the correlation function for short-term returns and an upper bound for long-term returns, a function that indicates how much the future returns are related to the past returns to a finite size region.

Other methods to calculate the correlation function from the PRTs were proposed in Refs. [10, 11]. One of the advantages of the proposed theoretical approach is that we could show, in a very trivial way, that if the distribution of the PRTs has an exponential decay then the correlation function also decays exponentially, a result rigorously demonstrated in [11].

Finally, in Sec. VII, we present our conclusions and discuss how this approach can be used in an integrated way to characterize experimental data coming from complex systems.

II. THE PROBABILITY DISTRIBUTION OF THE PRTS

In recent works [12, 13], it was shown that the fitted probability density function $\rho_F(\tau, \mathcal{B})$, of a series of Poincaré return times τ_n ($n = 1, \dots, L$) to a box \mathcal{B} of equal *finite* sides 2ϵ [14], of typical trajectories in a non-uniform hyperbolic attractor on \mathcal{R}^2 , deviates from the exponential law $\rho_P(\tau, \mathcal{B}) = \mu(\mathcal{B})e^{-\tau\mu(\mathcal{B})}$ if the box \mathcal{B} is placed on some special region of the phase space, where $\mu(\mathcal{B})$ is the probability measure inside it. This quantity measures the frequency with which a chaotic trajectory visits \mathcal{B} .

The function $\rho_P(\tau, \mathcal{B})$ describes well the discrete probability distribution function (PDF), denoted by $\rho(\tau, \mathcal{B})$, in Axiom-A systems and some classes of non-uniformly hyperbolic systems with exponential decay of correlations (=chaos with strong mixing properties) [15], for arbitrarily small intervals ($\epsilon \rightarrow 0$). In Ref. [13], it was hypothesized that for $\tau > \tau_{UPO}^{min}$, we have $\rho(\tau, \mathcal{B}) \rightarrow \rho'_F(\tau, \mathcal{B})$ with

$$\rho'_F(\tau, \mathcal{B}) = \beta e^{(-\alpha\tau)}, \quad (1)$$

where $\tau > \tau_{UPO}^{min}$ represents the PRT for which the distribution $\rho(\tau, \mathcal{B})$ becomes approxi-

mately continuous and $\beta = \beta_R + \alpha$. It was assumed that $\beta_R e^{(-\alpha\tau)}$ describes an effective PDF associated mostly with the return of trajectories along the unstable manifold of UPOs outside the box \mathcal{B} . It is the result of the non-hyperbolic nature of the dynamics inside the box, whose probability measure suffers the influence of non-local UPOs. The term $\alpha e^{(-\alpha\tau)}$ describes the hyperbolic nature of the dynamics inside the box, the return of trajectories to the box associated with the local dynamics provided by the UPOs inside the interval.

The coefficients of $\rho'_F(\tau, \mathcal{B})$ are obtained by the least square fitting method which minimizes the error between $\rho'_F(\tau, \mathcal{B})$ and $\rho(\tau, \mathcal{B})$:

$$E(\rho'_F - \rho) = (\rho'_F - \rho)^2. \quad (2)$$

In addition, assuming that Eq. (1) describes well $\rho(\tau, \mathcal{B})$, then the following equations should be simultaneously satisfied

$$\sum_{\tau_{min}}^{\tau_{UPO}^{min}} \rho(\tau, \mathcal{B}) + \int_{\tau_{UPO}^{min}}^{\tau_{max}} \rho'_F(\tau, \mathcal{B}) d\tau = 1 \quad (3)$$

$$\sum_{\tau_{min}}^{\tau_{UPO}^{min}} \rho(\tau, \mathcal{B}) \times \tau + \int_{\tau_{UPO}^{min}}^{\tau_{max}} \rho'_F(\tau, \mathcal{B}) \tau d\tau = \langle \tau \rangle \quad (4)$$

by considering that $\rho(\tau, \mathcal{B})$ can be broken in two terms, one that describes its discrete nature, the probability of finding a PRT of length $\tau < \tau_{UPO}^{min}$, and another that describes its continuous nature.

Denoting τ_{min} as to be the PRT with the minimum length $[\min(\tau_n)]$ and $\langle \tau \rangle = 1/L \sum_{n=1}^L \tau_n$, and assuming that $\tau_{min} = \tau_{UPO}^{min}$ then $\alpha \cong (\langle \tau \rangle - \tau_{min})^{-1}$ and $\beta_R \cong \alpha[e^{(\alpha\tau_{min})} - 1]$, for sufficiently small ϵ so that the terms that contain $\max(\tau_n)$, regarded as τ_{max} , can be neglected. So, for finite $\langle \tau \rangle$, $\beta > \alpha$. However, Eq. (1) does not seem to completely capture the nature of $\rho(\tau, \mathcal{B})$ for finite size intervals. Satisfying conditions (3) and (4) do not necessarily minimizes the error in (2), and the contrary also does not apply. Such disagreement becomes stronger in boxes centered close to homoclinic tangencies. By fitting $\rho(\tau, \mathcal{B})$ by a function of the type in Eq. (1) might produce $\beta \leq \alpha$, which disagrees with the inequality $\beta > \alpha$ that validates Eq. (1). For the here considered dynamical systems for parameters far away from intermittent behavior, and data coming from plasma turbulence and stock market [7], one finds often that $\alpha \cong \beta$, a consequence of $\rho(\tau, \mathcal{B})$ be greater than $\rho'_F(\tau, \mathcal{B})$, for $\tau < \langle \tau \rangle$, and that $\rho(\tau, \mathcal{B}) < \rho'_F(\tau, \mathcal{B})$, for $\tau > \langle \tau \rangle$. These facts suggest that

for systems with a dynamics similar to the Hénon map, the small term β_R considered to be constant in Ref. [13] is in fact a function that we hypothesize to be a power-law with respect to τ' . That lead us to

$$\rho_F(\tau', \mathcal{B}) = \left(\beta^* + c \left[1 - \left(\frac{\tau'}{\langle \tau_e \rangle} \right)^\gamma \right] \right) e^{(-\alpha\tau')} \quad (5)$$

where

$$\tau' = \tau - \tau_{UPO}^{min} + 1 \quad (6)$$

$$\langle \tau_e \rangle = \int_{\tau_{UPO}^{min}}^{\tau_{max}} \rho(\tau', \mathcal{B}) \tau' d\tau' \quad (7)$$

and γ is a positive small value. Notice that the use of τ' and $\langle \tau_e \rangle$ is only an artifact to simplify our further approximations and also to simplify any possible nonlinear fitting that we might make concerning the real PDF.

The power-law term $\beta_R = c[1 - (\frac{\tau'}{\langle \tau_e \rangle})^\gamma]$ shows that the considered systems for which this distribution holds have a return time distribution whose decay is not characterized by either a power-law or exponential decay but by both. It appears as a combined effect of the finiteness of the box, the expanding factor nearby low-periodic UPOs along the unstable direction, and the existence of homoclinic tangencies, which gives the non-uniformly hyperbolic character of the Hénon map and the Chua's circuit.

A large value of γ (which implies in a large β_R) indicates that there is a large contribution to the measure inside the box due to UPOs that are outside the box. Two things contribute for a large value of γ : the size and location of the box. The larger the size and the level of non-hyperbolicity of the box are, the larger the value of γ is. We find larger values of γ when we measure PRTs in boxes placed close to homoclinic tangencies. At such a case, trajectory points that have returned once to the box after P iterations keep consecutively returning to the box after P iterations. The trajectory is no longer under the influence of the linear expanding character of a period- P UPO (along the direction of the unstable eigenvector) but under the influence of the non-linear character of the unstable manifold of the UPO located outside the box.

A sketch of these ideas is depicted in Fig. 1. In (A), we represent a box that is centered on an UPO (in the figure represented by a full circle and the letter **O**). The box is sufficiently large so that the escape of trajectories from the box which are associated with this UPO happens no longer along the unstable eigenvector (E^u) but along the unstable manifold

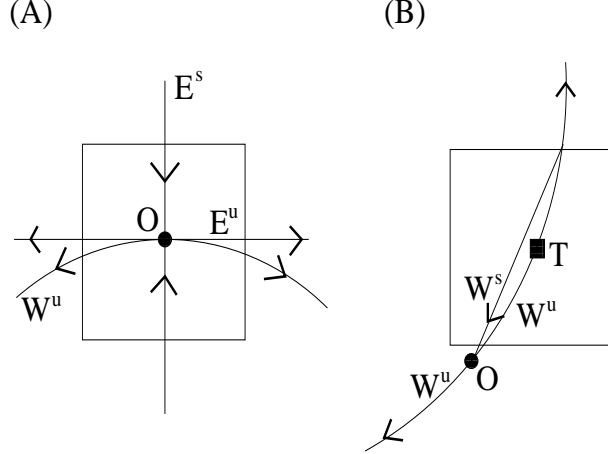


FIG. 1: A sketch of the structure of the manifolds and eigenvectors of UPOs (represented by full circles and the letter **O**) inside (A) or outside (B) a finite size box, where the PRTs are being measured. In (A), the box is far away from homoclinic tangencies, and in (B) the box is in the neighborhood of a homoclinic tangency (represented by the full square and the letter **T**).

(W^u). The smaller is the period of an UPO, the smaller is the eigenvalue of the unstable eigenvector. So, the escape of the trajectory along the unstable manifold is usually expected to happen for a low-period UPO. In (B), we represent a box centered in a homoclinic tangent (in the figure represented by a full square and the letter **T**). In the neighborhood of homoclinic tangencies exist low-period UPOs whose unstable and stable manifold happens to be almost parallel, forming a trapping region. In these trapping regions, the trajectory returns to the box along W^u and eventually escapes the box, but it may return to it along the stable manifold W^s of the UPO outside the box. For short returns, these confined trajectories contribute positively to $\rho(\tau, \mathcal{B})$, increasing $\mu(\mathcal{B})$.

We can classify regions \mathcal{B} by the way returns happen inside it: *type I* are the regions whose returns are associated with higher-period UPOs, here conveniently regarded as the hyperbolic ones. *type II and III* are the ones associated with lower-period UPOs, here conveniently regarded as the non-hyperbolic regions. In these regions, the deviation of $\rho_F(\tau, \mathcal{B})$ to the exponential is large, meaning a large γ . For the *type II* regions, the unusual returns that happen inside the interval are associated to UPOs outside it. Such behavior is a consequence of the existence of homoclinic tangencies [13] inside the region. For the *type III* regions, the unusual returns are associated with lower-period UPOs inside them. [13]. When there is an UPO with low period P inside the box, $\rho(\tau = P)$ is no longer exactly

equal to μ_{NR} [given by Eq. (A3)] due to the fact that linearization around this low-period UPO does not provide the measure due to this UPO inside the box.

III. ESTIMATION OF α , β^* , τ_{UPO}^{min} , ω , AND γ

To estimate α and β^* , we make $\gamma=0$ (treating the power-law term as a perturbation), and place $\rho_F(\tau, \mathcal{B})$ into Eqs. (3) and (4). We arrive that

$$\beta^* = \frac{\rho_e^2}{\langle \tau_e \rangle} \quad (8)$$

$$\alpha = \frac{\rho_e}{\langle \tau_e \rangle} \quad (9)$$

where $\rho_e(\mathcal{B}) = \int_{\tau_{UPO}^{min}}^{\tau_{max}} \rho(\tau, \mathcal{B}) d\tau$ and $\langle \tau_e \rangle$ defined as in Eq. (7).

As discussed in [13], the exponential part of the distribution reflects the stochastic nature of the returns associated with UPOs inside \mathcal{B} . It is interesting to know how much the exponential term $\beta^* \exp[-\alpha\tau']$ inside $\rho_F(\tau, \mathcal{B})$ deviates from the Poisson function $\frac{\mu}{1-\mu} \exp[\ln(1-\mu)\tau']$, a function that describes the probability with which returns happen if one considers trajectories generated by uncorrelated processes. For that, we calculate $\tilde{\mu}_1$ and $\tilde{\mu}_2$ such that

$$\frac{\tilde{\mu}_1}{1-\tilde{\mu}_1} \exp[\ln(1-\tilde{\mu}_2)\tau'] \cong \beta^* \exp[-\alpha\tau'] \quad (10)$$

We arrive that $\tilde{\mu}_1 \cong \frac{\beta^*}{1+\beta^*}$ and $\tilde{\mu}_2 \cong \alpha$. The continuous part of $\rho_F(\tau > \tau_{UPO}^{min})$ deviates from the Poisson distribution (for which $\tilde{\mu}_1 = \tilde{\mu}_2$) whenever $\tilde{\mu}_1 \neq \tilde{\mu}_2$. Such deviation becomes larger, the larger $|\mu - \alpha|$ ($= |\frac{\mu_e}{\rho_e} - \frac{\rho_e}{\langle \tau_e \rangle}|$, where $\mu_e(\mathcal{B}) = \mu(\mathcal{B})\rho_e(\mathcal{B})$). The larger $|\mu - \alpha|$ is, the larger $\tau_{UPO}^{min} - \tau_{min}$ (notice that $\mu = \alpha$ when $\tau_{min} = \tau_{UPO}^{min}$, what happens when $\epsilon \rightarrow 0$) and since α depends on τ_{UPO}^{min} it is reasonable to consider that the larger (the smaller)

$$\omega = (\tau_{UPO}^{min} - \tau_{min}) \quad (11)$$

is, the more correlated and deterministic (uncorrelated and stochastic) the returns are.

There are three approaches to estimate τ_{UPO}^{min} . One is by just inspecting when $\rho(\tau, \mathcal{B})$ presents a continuous exponential decay. The other is by fitting $\rho(\tau, \mathcal{B})$ considering an exponential function of the type $\rho'_F(\tau, \mathcal{B}) = \beta^* e^{-\alpha\tau}$, and τ_{UPO}^{min} is the value for which $[\rho'_F(\tau, \mathcal{B}) - \rho(\tau, \mathcal{B})]$ becomes smaller than some N/L ($N \in \mathbf{N}$, and L is the number of PRT observed). The last approach is the one that will be considered in this work due to its experimental orientation. For that one has just to notice that as τ becomes large, α as

estimated by Eq. (9) approaches an asymptotic value close to the value obtained by fitting $\rho(\tau, \mathcal{B})$ using the exponential function $\rho'_F(\tau, \mathcal{B})$.

To estimate γ , we consider that $\tau_{max} - \tau_{UPO}^{min} \gg 1$, and use that $[1 - (\frac{\tau'}{\langle \tau \rangle})^\gamma] \cong \gamma \ln(\frac{\langle \tau \rangle}{\tau'})$, $\alpha \approx \beta^*$, and $c \cong 1$ (so in the limit of $\epsilon \rightarrow 0$, $\rho_F(\tau', \mathcal{B}) \rightarrow \beta^* e^{-\alpha \tau'}$). Then, from Eq. (3) we arrive that

$$\gamma \propto \frac{\tau_{min}}{\log(\langle \tau \rangle) \langle \tau \rangle^2} \quad (12)$$

using that $\max(\tau'_{max}) \cong \tau_{max} \gg 1$. By making $\alpha \approx \beta^*$, we assume that the deviation of ρ_F from the exponential law ($\alpha e^{-\alpha \tau}$) is exclusively provided by the term β_R . In other words, the dynamical character of the system is provided by β_R . Therefore, manifestations of the deterministic behavior are more evident when $\frac{\tau'}{\langle \tau \rangle}$ is maximal and that happens for when $\tau' = 1$, what also means when $\tau = \tau_{min}$.

To simplify the presentation of our results, we rewrite Eq. (12) as

$$\gamma \propto \langle \tau \rangle^\theta \quad (13)$$

IV. KOLMOGOROV-SINAI ENTROPY

Now, we describe how the Kolmogorov-Sinai (KS) entropy can be written in terms of the PDF. Then, we apply this formalism to a typical physical situation when UPOs cannot be calculated and information about them is unknown.

Firstly, remind that by the Pesin's equality [16], the KS-entropy equals the sum of the positive Lyapunov exponents.

For uniformly hyperbolic systems [6] (see Appendix), it is valid to write that

$$\rho(\tau, \mathcal{B}) \cong \frac{N_{NR}(\tau, \mathcal{B})}{N(\tau)} \quad (14)$$

where $N_{NR}(\tau, \mathcal{B})$ and $N(\tau)$ represent the number of non-recurrent UPOs with period τ inside \mathcal{B} and $N(\tau)$ the total number of different UPOs of period τ embedded in the chaotic attractor. A non-recurrent UPO inside the region \mathcal{B} is an UPO that visits this region only once.

Also, for this class of systems, we can write that

$$N(\tau) = C \exp^{\tau \times H_{KS}} \quad (15)$$

where H_{KS} represents the Kolmogorov-Sinai entropy and C is a positive constant.

Then, placing Eq. (14) in (15), we have that $H_{KS} = -\frac{C}{\tau} + \frac{1}{\tau} \log \left[\frac{N_{NR}(\tau, \mathcal{B})}{\rho(\tau, \mathcal{B})} \right]$, in the limit of $\tau \rightarrow \infty$. Then, for a finite τ we have that

$$H_{KS}(\tau, \mathcal{B}) \leq \frac{1}{\tau} \log \left[\frac{N_{NR}(\tau, \mathcal{B})}{\rho(\tau, \mathcal{B})} \right] \quad (16)$$

As shown in Appendix A, it is reasonable to consider in Eq. (16) that $N_{NR} = 1$. Even if there are more than one non-recurrent UPO inside the region where the returns are being measured, making $N_{NR} = 1$ in Eq. (16) will not largely affect the estimation provided by this equation. So, to estimate the Lyapunov exponent of experimental systems, as the Chua's circuit, we will consider that

$$H_{KS}(\tau, \mathcal{B}) \leq \frac{1}{\tau} \log \left[\frac{1}{\rho(\tau, \mathcal{B})} \right] \quad (17)$$

This equation offers a way to estimate the KS-entropy of a chaotic system without having to calculate UPOs, a very difficult task.

Equation (16) is valid for uniformly hyperbolic systems of the class for which local quantities provide good approximations for global quantities (Tent map, for example). For the other types of uniformly hyperbolic systems and the non-uniformly hyperbolic systems (as the Logistic map, Hénon map, and Chua's circuit), the inequality in Eq. (16) should approximate well the divergence on initial conditions for trajectories departing from the considered region. Therefore, to obtain a good estimation of the Lyapunov exponent one should consider an average of this quantity taken over many regions in phase space as in

$$\langle H_{KS}(\tau) \rangle \leq \frac{1}{L} \sum_{k=1}^L \frac{1}{\tau} \log \left[\frac{N_{NR}(\tau, \mathcal{B}_k)}{\rho(\tau, \mathcal{B}_k)} \right] \quad (18)$$

where we are considering that this average is taken over \mathcal{B}_k regions in phase space, with $k = 1, \dots, L$.

Similarly, for experimental systems, we use

$$\langle H_{KS}(\tau) \rangle \leq \frac{1}{L} \sum_{k=1}^L \frac{1}{\tau} \log \left[\frac{1}{\rho(\tau, \mathcal{B}_k)} \right] \quad (19)$$

Let us now compare our result in Eq. (16) with a rigorous result [17] valid for a chaotic uniformly hyperbolic map (piecewise monotone maps of an interval with a finite number of branches and with bounded derivative of p -bounded variation with an invariant measures with positive entropy) that presents one positive Lyapunov exponent. For $\epsilon \rightarrow 0$, we have

that $\epsilon \cong \mu(\mathcal{B})$. From Kac's lemma we have that $\frac{1}{\langle \tau \rangle} = \mu(\mathcal{B})$ and then $\epsilon \cong \frac{1}{\langle \tau \rangle}$. Also, for a sufficiently small interval, $\rho(\tau_{min}, \mathcal{B}) \cong \mu(\mathcal{B})$ (assuming that $\rho(\tau, \mathcal{B})$ is well described by an exponential distribution), then Eq. (17) can be rewritten as $\lambda \cong \frac{-\ln(\epsilon)}{\tau_{min}}$, which agrees with the result derived in Ref. [17] that $\lambda = \frac{-\ln(\epsilon)}{\tau_{min}}$, for $\tau_{min} \rightarrow \infty$.

V. CORRELATION FUNCTION FOR SHORT-TERM RETURNS

The distribution $\rho(\tau, \mathcal{B})$ can be used to calculate the correlation function, a quantity that measures how fast a system loses information about the past as it evolves. Calling $\phi(x)$ to be some observable measured at the position x , the correlation between the observable ϕ at a time T [i.e., $\phi(F^T(x))$] with the initial observation $\phi(x)$ is given by [1]

$$C(\phi, T) = \int \phi(x)\phi(F^T(x))d\mu - \int \phi(x)d\mu \cdot \int \phi(F^T(x))d\mu \quad (20)$$

where $d\mu$ stands as usually to $\sigma(x)dx$ and $\sigma(x)$ represents the invariant density from which the invariant measure $\mu(\mathcal{B})$ can be calculated by $\mu(\mathcal{B}) = \int_{x \in \mathcal{B}} \sigma(x)dx$

In this work, we are mainly interested in understanding the behavior of the PRTs to regions \mathcal{B} . So, instead of averaging the correlation of trajectories over the whole space x , we calculate the correlation of trajectories in \mathcal{B} . Employing similar ideas to the ones in Refs. [6, 10, 18], and writing the observable to be $\mu(\mathcal{B})$, we have that

$$C(\tau, \mathcal{B}) = \mu[\mathcal{B} \cap F^{-\tau}(\mathcal{B})] - \mu[\mathcal{B}]\mu[F^{-\tau}(\mathcal{B})] \quad (21)$$

where $C(\tau, \mathcal{B})$ measures the correlation between trajectories that visit the region \mathcal{B} and that return to it after τ iterations. This function is also known as the speed of mixing.

For an invariant measure, we have that $\mu[\mathcal{B}] = \mu[F^{-\tau}(\mathcal{B})]$, and thus,

$$C(\tau, \mathcal{B}) = \mu[\mathcal{B} \cap F^{-\tau}(\mathcal{B})] - \mu[\mathcal{B}]^2. \quad (22)$$

The quantity $\mu[\mathcal{B} \cap F^{-\tau}(\mathcal{B})]$ represents the probability measure of having trajectory points leaving \mathcal{B} and returning to it after a series of returns τ_i , with $i = 1, \dots, l$ such that $\sum_i^l \tau_i = \tau$ and $\tau_i \leq \tau$. We can write the set $[\mathcal{B} \cap F^{-\tau}(\mathcal{B})]$ as a union of two sets $S' \cup S^*$ with $S' \cap S^* = \emptyset$, where S' as defined in Eq. (A5) and S^* defined as the set of points that are mapped to \mathcal{B} after τ iterations but with the additional fact that for each $x^* \in S^*$ **it exists** $\tau^* < \tau$ for

which $F^{\tau^*}(x^*) \in \mathcal{B}$. In other words, S^* represents the set of points that are mapped back to \mathcal{B} after τ iterations, excluding all the points that firstly return to \mathcal{B} after τ iterations.

If $\tau < 2\tau_{min}$, then, $\mu[\mathcal{B} \cap F^\tau(\mathcal{B})] = \mu(S')$. Using Eqs. (A4) and (A5), we arrive to that $\mu[\mathcal{B} \cap F^\tau(\mathcal{B})] = \mu(\mathcal{B})\rho(\tau, \mathcal{B})$, since there cannot be trajectory points that return more than once within this time interval.

Then, for $\tau < 2\tau_{min}$

$$C(\tau, \mathcal{B}) = \mu(\mathcal{B})\rho(\tau, \mathcal{B}) - \mu[\mathcal{B}]^2 \quad (23)$$

For $\tau > 2\tau_{min}$, we can always write that

$$C(\tau, \mathcal{B}) \leq \mu(\mathcal{B})\rho(\tau, \mathcal{B}) - \mu[\mathcal{B}]^2, \quad (24)$$

since $\mu[\mathcal{B} \cap F^\tau(\mathcal{B})] = \rho(\tau, \mathcal{B})\mu(\mathcal{B}) + \mu[S^*]$, Notice that as τ grows, $\mu[S^*] \rightarrow \mu_R$ in Eq. (A2).

Therefore, if the density of the returns has an exponential decay with respect to time, so will the correlation behave, a statement that was rigorously proved for some classes of systems and observables in Ref. [11]. The advantage of the approach proposed here is the simplicity with which we can understand such a rigorous result.

From Eqs. (23) and (24) we can clearly see that the larger $(\rho(\tau, \mathcal{B}) - \mu[\mathcal{B}])$ is, the slower the decay of the correlation function. That is exactly the case for type II and III non-hyperbolic regions, for $\tau < 2\tau_{min}$, when the distribution $\rho(\tau, \mathcal{B})$ receives a large contribution of the power-law term β_R . For the type I hyperbolic regions, $C(\tau, \mathcal{B})$ decays much faster to 0, since $\rho(\tau, \mathcal{B}) \approx \mu(\mathcal{B})$. And typically, the bigger ω in Eq. (11) is, the bigger $(\rho(\tau, \mathcal{B}) - \mu[\mathcal{B}])$. That is so because the smaller τ_{min} is, the larger $\rho(\tau_{min}, \mathcal{B})$.

In Ref. [6], a similar derivation of the correlation function was proposed, but considering the correlation between trajectories departing from S' and arriving to \mathcal{B} . In other words, the correlation between trajectories that produce first returns and that return only once to \mathcal{B} . In Eqs. (23) and (24), one can estimate the correlation between all trajectories departing from \mathcal{B} and arriving in \mathcal{B} including also trajectories that return more than once.

VI. DETERMINISM AND STOCHASTICISM IN THE HÉNON MAP AND THE EXPERIMENTAL CHUA'S CIRCUIT

The Hénon's map is given by $x_{n+1} = a - x_n^2 + by_n$, and $y_{n+1} = x_n$, with $a = 1.4$ and $b=0.3$, and the considered experimental Chua's circuit can be seen in Ref. [19]. We focus

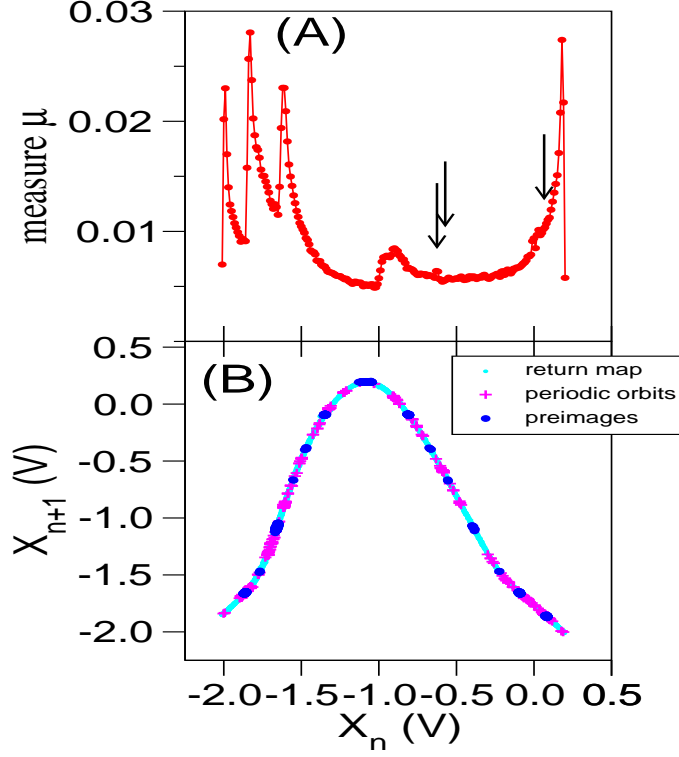


FIG. 2: [Color online] Results from the experimental Chua’s circuit. (A) Probability measure with which X_n visits intervals of length $\epsilon = 0.005V$. The arrows (from left to right) indicate the intervals \mathcal{B}_1 , \mathcal{B}_3 , and \mathcal{B}_2 , respectively. (B) First returning map $X_n \times X_{n+1}$ in full gray squares, pre-images of trajectory points located at the maximum of the returning map in stars, and the UPOs of up to period 6 in pluses.

our analyzes in three regions \mathcal{B}_1 (type I), \mathcal{B}_2 (type II), and \mathcal{B}_3 (type III).

For the Hénon attractor, the regions \mathcal{B} are boxes of equal sides 2ϵ . The region \mathcal{B}_1 represents a box centered at $(x, y) = (1.11807, 0.14719)$, \mathcal{B}_2 a box centered at the primary homoclinic tangent $(x, y) = (1.780098, 0.09495)$, and \mathcal{B}_3 a box centered at a period-2 UPO $(x, y) = (1.36612008, -0.666120078)$.

For the Chua’s circuit, we reconstruct the attractor using the same techniques of Ref. [19] and make the trajectory discrete, producing a discrete time series represented by X_n , which represents the voltage in the capacitor C_1 , whenever the voltage in the capacitor C_2 reaches zero. The attractor is of the Rössler-type. In Fig. 2(A) we show the invariant measure of X_n and in 2(B), the first returning map $X_n \times X_{n+1}$, by the gray full squares. The (blue) stars represent trajectory points located at the maximum of the return map and its pre-images.

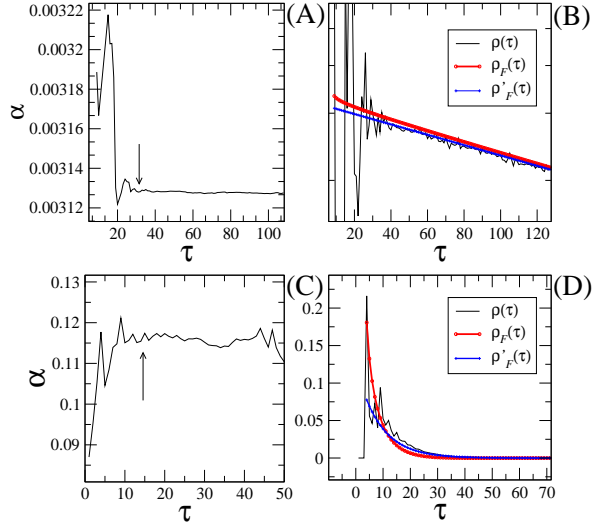


FIG. 3: [Color online] (A) and (B) are results for the Hénon attractor and (C) and (D) results for the experimental Chua's circuit. Estimation of the parameter α and τ_{UPO}^{min} for the Hénon attractor (A) and for the Chua's circuit (C). In (B) and (D), we show $\rho(\tau, \mathcal{B})$, the fitting of $\rho(\tau, \mathcal{B})$ by a function of the type $\rho_F(\tau, \mathcal{B})$ [Eq. (5)], and the fitting of $\rho(\tau, \mathcal{B})$ by an exponential function of the type $\rho'_F(\tau, \mathcal{B})$ [Eq. (1)]. The fittings are made by considering the transformed time τ' [Eq. (6)] but, in these figures, we re-transform the time back to τ in order to plot the fittings together with the distribution $\rho(\tau, \mathcal{B})$.

Every pre-image is located at a X_n point for which the probability density is large in (A), what typically happens for non-uniformly hyperbolic systems. The plus symbol indicates the place of the lower-period UPOs (up to period 6). In this circuit, \mathcal{B} represents intervals of size ϵ . \mathcal{B}_1 represents the interval centered at $X_n = -0.64$, \mathcal{B}_2 the interval centered at $X_n = 0.05$, and \mathcal{B}_3 the interval centered at the position of a period-2 UPO $X_n = -0.586637$. These points where the intervals are positioned are indicated by the arrows in Fig. 2(A).

We now make a detailed analysis of the PRTs to the box \mathcal{B}_2 , for the Hénon map [in Figs. 3(A-B)], and the PRTs to the interval \mathcal{B}_2 , for the Chua's circuit [in Figs. 3(C-D)]. In (A) and (C), we estimate the value of α as we consider different values for τ_{UPO}^{min} , in Eq. (9). We consider the smallest value of τ_{UPO}^{min} for which the value of α "converges". The arrow indicates these values. For the Hénon attractor, $\tau_{UPO}^{min} = 28$ and for the Chua's circuit, $\tau_{UPO}^{min} = 13$. In (B) and (D), we show $\rho(\tau, \mathcal{B})$, $\rho_F(\tau, \mathcal{B})$, and a fitting of $\rho(\tau, \mathcal{B})$ by an exponential function of

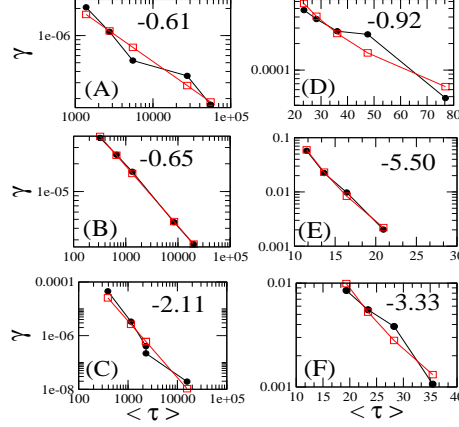


FIG. 4: The fittings of γ (vertical axis) versus $\langle \tau \rangle$ in a log-log graph, for the distributions ρ_F of Hénon map in (A-C) (left column) and for the experimental Chua's circuit in (D-F) (right column), in the form $\gamma \propto \langle \tau \rangle^\theta$ [see Eq. (13)]. The value of the power θ is shown inside the figures. Experimentally, the value of $\langle \tau \rangle$ is over-estimated, which leads to a smaller θ exponent.

the type of $\rho'_F(\tau, \mathcal{B})$ [Eq. (1)]. For the Hénon attractor (B), using the distribution $\rho_F(\tau, \mathcal{B})$ in the integral of Eq. (3) produces the value 0.994826 while using $\rho'_F(\tau, \mathcal{B})$ produces 0.987701. For the Chua's circuit (D), using the distribution $\rho_F(\tau, \mathcal{B})$ in the integral of Eq. (3) produces the value 0.78 while using $\rho'_F(\tau, \mathcal{B})$ produces 0.68. Reminding that the integrals in Eq. (3) should provide 1, it is clear that the proposed distribution in Eq. (5) fits better $\rho(\tau, \mathcal{B})$.

In Fig. 4, we show the relation between γ and $\langle \tau \rangle$ for \mathcal{B}_1 , \mathcal{B}_2 , and \mathcal{B}_3 , in the Hénon attractor [first column, (A-C)] and in the Chua's circuit [second column, (D-F)]. We have numerically obtained that for the Hénon map, $\gamma \propto \langle \tau \rangle^\theta$ with $\theta \cong -0.6$ [excluding the region \mathcal{B}_3 , whose results are shown in (C)], and for the Chua's circuit $\gamma \propto \langle \tau \rangle^\theta$ with $\theta < -0.9$. Remind that the larger is $|\theta|$, the smaller β_R .

For type II non-hyperbolic regions, as ϵ is decreased, typically we expect that the unstable manifold of the UPO outside the region will still belong to the region, which leads to a small $|\theta|$ value.

Table I shows estimates for the positive Lyapunov exponent using the right-hand side of Eq. (16) for the Hénon map and Eq. (17) for the Chua's circuit. \mathcal{B}_1 represents a hyperbolic type I region and \mathcal{B}_2 a non-hyperbolic type III region, with different sizes ϵ .

TABLE I: Estimation of the Lyapunov exponent. For the Hénon map, we typically find that the UPO with the smallest period has a period larger than the observed τ_{min} , a consequence of the non-hyperbolic character of this map [see Fig. 6(B) and 6(D)]. Thus, for calculating the Lyapunov exponent, we consider in Eq. (16) $\tau = P_{min}$, where P_{min} is the lowest period of all UPOs inside \mathcal{B} . For all regions studied in this map, the number of non-recurrent UPOs is within the interval $N_{NR} = [1, 2]$ as expected. For the experimental Chua’s circuit, we calculate the Lyapunov exponent considering in Eq. (17) τ equal to the first Poincaré return for which the PDF presents its third maximum. We also assume that $N_{NR} = 1$. The positive Lyapunov exponent of the Hénon attractor is also calculated using the technique in Ref. [16] and the largest Lyapunov exponent of the Chua’s circuit is also calculated using the technique in Ref. [20], with the code of the Tisean package [21]. We obtain that the positive Lyapunov exponent of the Hénon map is 0.419/iteration and the one for the Chua’s circuit is 0.52/cycle. The value of τ used is the number between parentheses.

ϵ - Hénon	0.02	0.01	0.005	0.001	0.0008
\mathcal{B}_1	0.32(21)	0.40(23)	0.40(23)	0.39(23)	0.39(23)
\mathcal{B}_2	0.61(18)	0.33(18)	0.36(18)	0.40(22)	0.29(29)
ϵ - Chua	0.1700	0.1450	0.1200	0.0950	0.0700
\mathcal{B}_1	0.43(7)	0.42(7)	0.42(7)	0.42(7)	0.46(9)
\mathcal{B}_2	0.58(5)	0.39(7)	0.58(5)	0.25(13)	0.27(13)

For the Hénon attractor, a numerical calculation of this exponent provides $\lambda=0.419$ [16], and for the experimental Chua’s circuit, $\lambda=0.52/\text{cycle}$ [20, 21]. The unit of the Lyapunov exponent for this circuit is in [1/cycles]. That is due to the fact that for the calculation of this exponent we have used the discrete time series X_n , which represents the voltage in capacitor C_1 whenever the voltage of capacitor C_2 is zero.

In both systems, the Lyapunov exponents estimated from Eqs. (16) [for the Hénon map] and (17) [for the Chua’s circuit] using returns measured in the non-hyperbolic regions \mathcal{B}_2 produce worse estimates than the ones measured in the hyperbolic regions \mathcal{B}_1 . That is to be expected since our estimations are valid for uniformly hyperbolic systems. For both systems and all regions, the estimation of the Lyapunov exponents produce better results as the size of the regions decrease and τ_{min} becomes large. That is also to be expected since as the size of the box decreases the chance that a region has a hyperbolic character increases.

Since both the Hénon map and the Chua's circuit are non-uniformly hyperbolic systems, in order to obtain better estimates for the Lyapunov exponents we need to calculate an average value considering many regions in phase space.

To firstly illustrate how an average value provides a better estimation for the real value of the Lyapunov exponent, we average all the values shown in Table I. For the Hénon map, we obtain that $\lambda = 0.39$ (the real Lyapunov exponent is 0.419) and for the Chua's circuit we obtain that $\lambda = 0.42$ (the real value is 0.52).

Then, we calculate $\langle H_{KS} \rangle$ for the Hénon map, using Eq. (18) and considering $L = 500$ regions with $\epsilon = 0.005$ and $\tau = P_{min}$, where P_{min} is the lowest period of all UPOs inside each region. We obtain that $\langle H_{KS} \rangle = 0.464$ (compare with the real value 0.419). These $L = 500$ regions are centered in points of a 500 long trajectory. Using Eq. (19) for the same previous conditions, we obtain $\langle H_{KS} \rangle = 0.441$. For the Chua's circuit, we calculate $\langle H_{KS} \rangle$ using Eq. (19) considering $L = 25$ regions \mathcal{B} with $\epsilon = 0.067$ and τ equal to the second largest first Poincaré return. We obtain that $\langle H_{KS} \rangle = 0.42 \pm 0.1$ (compare with the real value 0.52).

In Fig. 5, we show the decay of the correlation function with respect to τ . Notice that this function is local and reflects the decay of correlation of PRTs to a particular interval. As expected, the correlation function decays faster in the type I hyperbolic regions [(A) and (C)] than in the type II non-hyperbolic regions. In addition, in general, the larger ϵ is, the larger the value of the correlation function, a consequence of the fact that the larger ϵ is, the larger both θ and ω are.

VII. CONCLUSIONS

We have studied the Poincaré recurrence time (PRT) of chaotic systems, a quantity that measures the time interval between two consecutive visits of a trajectory to a finite size region in phase space. The motivation in studying PRT is that for some systems the only possible measure one can make is the time interval between two events. But one still wants to understand what kind of dynamics is behind the generation of these returns.

If the region in phase space has an arbitrarily small size, for systems that have strong mixing characteristics, a long return time contains no longer information about the future returns, which means that the consecutive series of returns lose their correlation and they behave as if they had been generated by a completely random process. At such a situation,

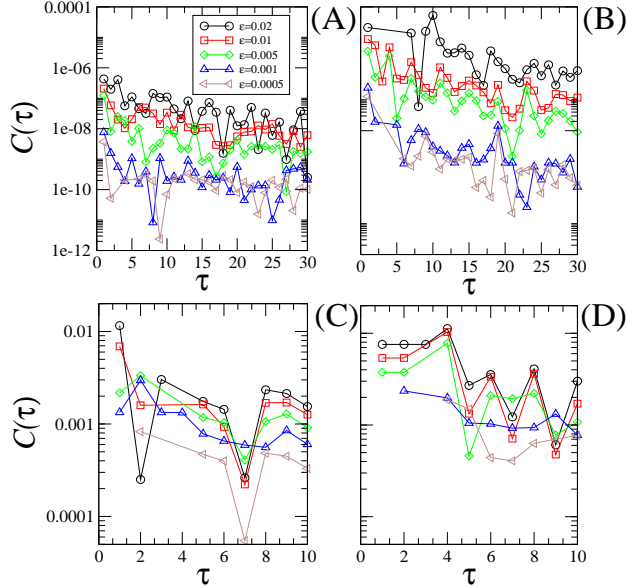


FIG. 5: Correlation function with respect to τ for the Hénon map (A-B) and the experimental Chua's circuit (C-D). In (A) and (C), we consider the type I hyperbolic regions \mathcal{B}_1 , and in (B) and (D), we consider the type II non-hyperbolic regions \mathcal{B}_2 .

the probability distribution of the PRTs approaches a Poisson distribution [15, 22] and few can be said about the dynamical manifestations of the data by only considering the form of this distribution.

Our approach is mainly devoted to characterize a chaotic system (obtaining relevant invariant quantities) considering regions with finite size and short return times. We show how to calculate the short-term correlation function [see Eq. (23)] and the Kolmogorov-Sinai entropy [see Eqs. (17) and (19)], using the distribution of PRTs, a quantity that can be easily accessible in experiments.

As the region in phase space where the returns are being measured becomes larger, the first Poincaré returns reflect more the deterministic nature of the system. That leads to a large deviation of the density of the returns from the Poisson [see Eq. (5)] and a slower decay of correlations for short-term returns [see Eq. (23) and Fig. 5].

These characteristics can be advantageously used to characterize the level of determinism in chaotic systems. More specifically, the larger θ is in Eq. (11), the more deterministic is the considered chaotic system under the point of view of the PRTs. Another quantity is $\omega = \tau_{UPO}^{min} - \tau_{min}$, where τ_{UPO}^{min} is the return value for which the probability distribution

of the PRTs presents a continuous decay with the increasing of the return time, and τ_{min} is the return with the minimal length. The larger ω is, the larger is the time span within which discontinuities are observed in the distribution of returns. Each discontinuity identifies particular returns, which makes them to be highly predictable. As shown in Sec. V, these previous intuitive ideas are indeed correct, i.e., larger θ and ω result in a slower decay of correlations.

The strategy of using a value of τ that is larger than τ_{min} in Eqs. (18) and (19) is due to the fact that in non-hyperbolic systems as the Hénon map and the experimental Chua's circuit the density of the PRTs for $\tau = \tau_{min}$, i.e. $\rho(\tau_{min}, \mathcal{B})$, receives a contribution coming from UPOs outside of \mathcal{B} , which violates the conditions under which these equations are derived. When the UPOs are known as it is the case for the Hénon map, we use $\tau = P_{min}$, in Eqs. (18) and (19), where P_{min} represents the period of the UPO inside \mathcal{B} with the lowest period. When the UPOs are unknown as it is the case for the experimental Chua's circuit, we use $\tau > \tau_{min}$.

Our approach can be straightforward applied to the treatment of data coming from complex systems, and the reason lies on the formulas that we have used. As one can check the 3 most relevant formulas used in our work [Eqs. (11), (19), and (23)] depend only on the probability of the Poincaré return times to finite size intervals with short time-length, a quantity that can be easily and quickly accessible from measurements and that, in principle, does not require the existence of chaos.

For some technological applications as in the control of chaos [23], one does not need to know with high precision the position of an UPO, but rather its unstable eigenvalue. Equation (A8) offers a trivial way to calculate this quantity by measuring the probability with which the fastest first Poincaré return to a sufficiently small interval happens. Naturally, this equations also offers a simple way to obtain estimations for the local first derivative of a system, a quantity often needed to make local models of complex systems. If the system is higher-dimensional then L_{min} in Eq. (A8) should refer to the product of all the unstable eigenvalues of a single non-recurrent UPO appearing in the region, as explained in Ref. [24].

Acknowledgments: MSB would like to thank the wonderful discussions with Benoit Saussol, Miguel Mendes, and Tomas Persson, during the International conference in honor of Yakov Pesin on his 60th birthday (25-29 June, 2007), concerning the Poincaré return time to regions of finite size, discussions which partially influenced the many ideas presented in

this work, and also discussions with M. Todd about recent mathematical proofs concerning the exponential statistics of the PRTs. MSB was also partially supported by the Centro de Matemática da Universidade do Porto, financed by FCT through the programmes POCTI and POSI, with Portuguese and European Community structural funds. JCS and DMM acknowledge the financial support of CNPq and FAPESP.

- [1] M. Viana, Stochastic dynamics of deterministic systems, Brazillian Math. Colloquium IMPA, 1997; A. Lacosta, M. C. Mackey, Chaos, Fractals, and noise, Springer, 1994.
- [2] K. T. Alligood, T. D. Sauer, J. A. Yorke, Chaos, an introduction to dynamical systems, Springer, 1997; H. Kantz and T. Schreiber, Nonlinear time series analysis, Cambridge University Press, Cambridge, 1997.
- [3] C. Komalapriya, M. Thiel, M. C. Romano, *et al.*, Reconstruction of a system's dynamics from short trajectories, Phys. Rev. E, 78 (2008) 066217 (2008).
- [4] G. Nicolis and C. Rouvas-Nicolis, in Encyclopedia of Nonlinear Sciences, Routledge, New York, 2005.
- [5] H. Poincaré, Sur le problme des trois corps et les équations de la dynamique, Acta Mathematica, 13 (1890), 1-270.
- [6] P. R. F. Pinto, M. S. Baptista, I. Labouriau, First Poincaré return, natural measure, UPO and Kolmogorov-sinai Entropy, arXiv:0908.4575.
- [7] M. S. Baptista, I. L. Caldas, M. V. A. P. Heller, and A. A. Ferreira Recurrence in plasma edge turbulence, Phys. Plasmas, 8 (2001), 4455-4462; M. S. Baptista and I. L. Caldas, Stock Market Dynamics, Physica A, 312 (2002) 539-564.
- [8] P. Grassberger and I. Procaccia, Estimation of the Kolmogorov entropy from a chaotic signal Phys. Rev. A 28, (1983), 2591-2593.
- [9] A. Cohen and I. Procaccia, Computing the Kolmogorov entropy from time signals of dissipative and conservative dynamical systems, Phys. Rev. A, 31 (1985) 1872-1882.
- [10] R. Artuso, Correlation decay and return time statistics, Physica D, 131 (1999), 68-77.
- [11] L.-S. Young, Recurrence times and rates of mixing, Israel Journal of Mathematics, 110, (1999), 153-188.
- [12] Eduardo G. Altmann, Elton C. da Silva, and Iberê L. Caldas, Recurrence time statistics for

- finite size intervals, *Chaos*, 14 (2004), 975-981.
- [13] M. S. Baptista, S. Kraut, C. Grebogi, Poincaré recurrence and measure of hyperbolic and nonhyperbolic chaotic attractors, *Phys. Rev. Lett.*, 95, (2005) 094101.
- [14] The Poincaré return time (PRT) is the number of iterations needed to make a trajectory leaving from a point in the attractor inside a region to return to it. A typical trajectory generates a series of returns $\tau_1, \tau_2, \dots, \tau_L$.
- [15] B. Saussol, On fluctuations and the exponential statistics of return times *Nonlinearity*, 14 (2001), 179-191; M. Hirata, B. Saussol, and S. Vaienti, Statistics of return times: a general framework and new applications, *Comm. Math. Phys.* 206, (1999), 33-55.
- [16] J.-P. Eckmann and D. Ruelle, Ergodic theory of chaos and strange attractors, *Rev. Mod. Phys.* 57 (1985) 617-656.
- [17] B. Saussol, Recurrence rate in rapidly mixing dynamical systems, *Discrete and Continuous Dynamical Systems A*, 15 (2006), 259-267.
- [18] B. V. Chirikov, D. L. Shepelyansky, Correlation properties of dynamical chaos in Hamiltonian systems, Ninth International Conference of Nonlinear Oscillations, Kiev 1981, Naukova Dumka, Kiev, 1984, vol. II; B. V. Chirikov, D. L. Shepelyansky, Correlation properties of dynamical chaos in Hamiltonian systems, *Physics D*, 13, (1984) 395-400; C. F. F. Karney, Long-time correlations in the stochastic regime, *Physica D*, 8 (1983) 360-380.
- [19] D. M. Maranhão, M. S. Baptista, J. C. Sartorelli, I. L. Caldas, Experimental observation of a complex periodic window, *Phys. Rev. E.*, 77 (2008) 037202.
- [20] M. Sano and Y. Sawada, Measurement of the Lyapunov spectrum from a chaotic time series *Phys. Rev. Lett.*, 55 (1985) 1082-1085.
- [21] R. Hegger, H. Kantz, and T. Schreiber, Practical implementation of nonlinear time series methods: the TISEAN package, *Chaos*, 9 (1999) 413.
- [22] P. Collet, Some ergodic properties of maps of the interval, Lectures given at the CIMPA summer school, *Dynamical Systems and Frustrated Systems*, Hermann, Paris, 1996.
- [23] E. Ott, C. Grebogi, and J. A. Yorke, Controlling chaos, *Phys. Rev. Lett.* **64**, (1990) 1196-1199.
- [24] C. Grebogi, E. Ott, J. A. Yorke, Unstable periodic orbits and the dimensions of multifractal chaotic attractors, *Phys. Rev. A*, 37, (1988) 1711-1724.
- [25] Y.-C. Lai, Y. Nagai, and C. Grebogi, Characterization of the Natural Measure by Unstable Periodic Orbits in Chaotic Attractors, *Phys. Rev. Lett.* **79**, 649 (1997).

[26] L. Perko, Differential Equations and Dynamical Systems (Springer-Verlag, New York, 1991).

APPENDIX A: THE DENSITY OF RETURNS ρ AND THE NON-RECURRENT UPOS

In Ref. [24] it is derived a formula that relates the probability measure of a D -dimensional box \mathcal{B} with the unstable eigenvalues of the UPOs inside it. More specifically,

$$\mu(\mathcal{B}) = \lim_{P \rightarrow \infty} \left[\sum_j L_j(P)^{-1} \right] \quad (\text{A1})$$

where $L_j(P) = L_{1j}(P)L_{2j}(P)\dots L_{Uj}(P)$, and $L_{uj}(P)$ ($u = 1, \dots, U$) represent the U positive eigenvalues (larger than 1) of the j fixed point located in \mathcal{B} of the P -fold iterate of the map represented by F^P (i.e., the fixed points are period- P UPOs that belongs to \mathcal{B}), where P tends to infinity. In a general situation, there are U positive eigenvalues and the box is D -dimensional. In the following, we consider $D=2$, and $U=1$ (there is only one positive Lyapunov exponent).

Equation (A1) was demonstrated to hold for mixing hyperbolic (axiom A) attractors and was shown numerically to hold for the non-hyperbolic Hénon attractor in Refs. [13, 25], for UPOs of moderately large period $P \cong 30$.

As done in Ref. [6], we rewrite the right-hand side of Eq. (A1) as a sum of two terms, without taking the limit of $P \rightarrow \infty$ but for a finite P :

$$\sum_j L_j(P)^{-1} = \mu_R + \mu_{NR} \quad (\text{A2})$$

where $\mu_R = \sum_j [L_j^R(P)]^{-1}$ and

$$\mu_{NR} = \sum_j [L_j^{NR}(P)]^{-1}, \quad (\text{A3})$$

where $L_j^R(P)$ are the unstable eigenvalues of the so called *recurrent* UPOs that return to \mathcal{B} more than once before completing their cycles, and $L_j^{NR}(P)$ are the unstable eigenvalues of the so called *non-recurrent* UPOs that return to \mathcal{B} only once. So, while μ_{NR} measures the contribution to the measure due to chaotic trajectories associated with non-recurrent UPOs, μ_R measures the contribution to the measure due to chaotic trajectories associated with recurrent UPOs.

As shown in Ref. [6], there is a clever way to relate the density $\rho(\tau, \mathcal{B})$ with the measure of the attractor associated with UPOs inside \mathcal{B} by

$$\rho(\tau, \mathcal{B}) = \mu_{NR}(\tau, \mathcal{B}) \quad (\text{A4})$$

The term $\mu_{NR}(\tau, \mathcal{B})$ can be represented in terms of space averages by

$$\mu_{NR}(\tau, \mathcal{B}) = \frac{\mu(S')}{\mu(\mathcal{B})} \quad (\text{A5})$$

where $\mu(S')$ represents the measure of the set S' (the part of the measure inside \mathcal{B} due to the set S') and S' represents the set of points of the attractor that returns firstly to \mathcal{B} after τ iterations. More rigorously, representing by F the transformation that generates a chaotic set A and given a subset $\mathcal{B} \subset A$, then $S' \in A$ and $S' = F^{-\tau}(\mathcal{B}) \cap \mathcal{B}$ such that there is not $\tau^* < \tau$ for which $F^{\tau^*}(\mathcal{B}) \cap \mathcal{B} \neq \emptyset$.

But the right-hand side of Eq. (A5) can be estimated by $\frac{N_{NR}(\tau, \mathcal{B})}{N(\tau)}$, and therefore,

$$\mu_{NR}(\tau, \mathcal{B}) = \frac{N_{NR}(\tau, \mathcal{B})}{N(\tau)}, \quad (\text{A6})$$

where $N_{NR}(\tau, \mathcal{B})$ and $N(\tau)$ represent the number of non-recurrent UPOs with period τ inside \mathcal{B} and $N(\tau)$ the total number of different UPOs of period τ embedded in the chaotic attractor.

Now, using Eq. (A3), it is clear that

$$\rho(\tau, \mathcal{B}) \geq L_{min}(\tau)^{-1}, \quad (\text{A7})$$

where L_{min} represents the unstable eigenvalue with the lowest amplitude within all UPOs with period τ .

In Fig. 6, we show the values of $L_{min}(\tau)^{-1}$ and the density of returns ρ in the Hénon attractor, for the regions \mathcal{B}_1 [in (A)], \mathcal{B}_2 [in (B)], \mathcal{B}_3 [in (C)], and also for a region centered at a period-8 UPO [in (D)] at the position $(x, y) = (1.496703, -0.545333)$, denoted by \mathcal{B}_4 .

We see that for $\tau \cong \tau_{min}$, inequality in Eq. (A7) is close to an equality and we can write that

$$\rho(\tau_{min}, \mathcal{B}) \cong L_{min}(\tau_{min})^{-1}. \quad (\text{A8})$$

The reason is that for such a case, there is only a few (a number of the order of 1) non-recurrent UPOs with period τ_{min} . It is easy to understand that by using the following

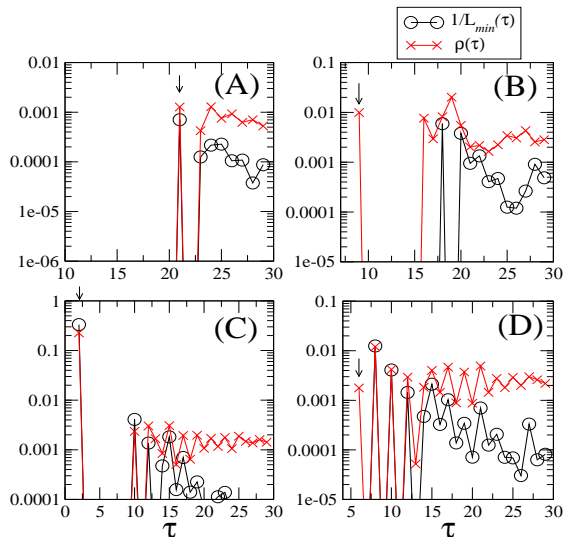


FIG. 6: By empty circles we show $1/L_{min}(\tau)$ and (red) crosses the value of $\rho(\tau, \mathcal{B})$, for the Hénon attractor for different regions. \mathcal{B}_1 [in (A)], \mathcal{B}_2 [in (B)], and \mathcal{B}_3 [in (C)], and also for a region centered at a period-8 UPO [in (D)]. $\epsilon = 0.02$ in all figures. The arrow points to the value of τ_{min} .

argument. Imagine a sufficiently small region centered around an UPO with period $P = 1$. Clearly $\tau_{min} = 1$ and there will be only one non-recurrent UPO with period $P=1$. Now, consider a region around an UPO with period $P=2$. Similarly, $\tau_{min} = 2$ and there will be only one UPO with period 2. Typically, for sufficiently small regions, there will be only one non-recurrent UPO inside the regions if $P \cong \tau_{min}$.

Provided that the UPO is hyperbolic, the uniqueness of the UPO in the small region is guaranteed by the Hartman-Grobman Theorem [26] and the size of the region in which the uniqueness of the UPO can be guaranteed is related to the strength of the hyperbolicity of the UPO.

To illustrate that, we consider the Logistic map $[x_{n+1} = bx_n(1 - x_n)]$, whose bifurcation diagram is shown in Fig. 7(A), constructed considering 100 parameter values b within the parameter range $[3.6, 3.99]$. In Fig. 7(B), we show the number of non-recurrent UPOs, denoted by N_{NR} , for UPOs with period $P = \tau_{min}$ and intervals with size $\epsilon = 0.001$, randomly selected such that $\tau_{min} \in [10, 14]$. For the large majority of intervals, $N_{NR} = 1$. Finally, in 7(C), we show the values of $\langle H_{KS} \rangle$ calculated from Eq. (19) for this parameter range. Notice that despite the choice of $N_{NR} = 1$, the value of $\langle H_{KS} \rangle$ is a good estimation for the

positive Lyapunov exponent of this map, indicated in this figure by λ .

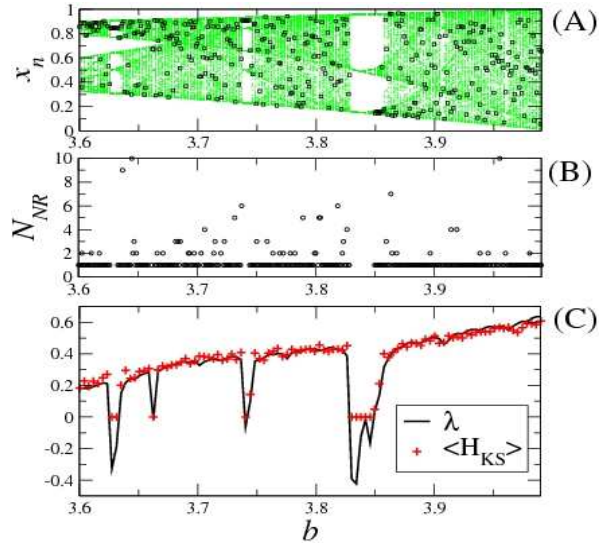


FIG. 7: [Color online] Results for the Logistic map: $x_{n+1} = bx_n(1 - x_n)$. (A) Bifurcation diagram of the Logistic map (green points). Empty squares represent intervals of size $\epsilon = 0.001$ randomly selected such that $\tau_{min} \in [10, 14]$. We consider 100 parameter values within the range $[3.6, 3.99]$ and for each parameter we consider one interval. (B) the number N_{NR} of non-recurrent UPOs with period $P = \tau_{min}$ inside each one of the 100 intervals. (C) The value of the Lyapunov exponent (black tick line), denoted by λ , and $\langle H_{KS} \rangle$ (red pluses) calculated from Eq. (19).